Wakefield Simulation of Solid State

Sahel Hakimi, Tam Nguyen, Deano Farinella, Calvin K. Lau, Hsuan Wang, Peter Taborek, Toshiki Tajima
University Of California, Irvine, Irvine, 92697

Motivation

- Traditional particle acceleration technology has an acceleration gradient limit of approximately 1MeV/cm due to material breakdown
- The alternative technique of laser wakefield acceleration (LWFA) uses plasma as the accelerating medium and is capable of producing higher acceleration gradients compared to traditional accelerators
- Electron Energy gain in 1D LWFA is given by: $\epsilon = 2a_0^2 m_e c^2 (\frac{n_{cr}}{ne})$
- Acceleration length is given by: $L_{acc} = a_0 \left(\frac{c}{\omega_{pe}}\right)\left(\frac{\omega_l}{\omega_{pe}}\right)^2 \propto \left(\frac{n_{cr}}{n_e^{3/2}}\right)$
- In the past, increasing the energy gain has been carried out by decreasing the plasma density
  - Acceleration length will increase as well
  - Laser energy must be increased
- Increasing the energy gain is also possible by increasing n_{cr} through increasing the laser frequency
  - We need X-ray lasers
- Recent advancement in laser technology known as the Thin Film Compression[1] allows us to consider LWFA in the X-ray regime and with solid densities[2]
- For current optical lasers and gaseous plasmas, the typical ratio is $\frac{n_{cr}}{n_e} = \frac{10^{21}\text{cm}^{-3}}{10^{18}\text{cm}^{-3}} = 10^3$, whereas for an X-ray laser and a solid density plasma, we could for example have $\frac{n_{cr}}{n_e} = \frac{10^{29}\text{cm}^{-3}}{10^{23}\text{cm}^{-3}} = 10^6$, three orders of magnitude higher

What is new?

- Previous simulations confirmed an accelerating gradient of TeV/cm when the wakefield is driven by an X-ray laser compared to GeV/cm for when it is driven by an optical laser[4]
- High energy X-ray photons can couple with ionic motions through optical phonon modes[3] (polariton effects)
- We include the **polariton effects** in our 1D simulations
- $\epsilon(k,\omega) = 1 - \frac{\omega_{pi}^2}{\omega^2-\omega_{TO}^2} - \frac{\omega_{pe}^2}{\omega^2-k_x^2v_e^2}$, where $\omega_{TO} = \sqrt{\frac{K_i}{m_i}}$

Derivation

- The dispersion relation can be derived from the fluid moment equations. Basic equations for this setup are the (1D) continuity and momentum equations for both species and Poisson's equation:

$$\frac{\partial n_e}{\partial t} + \nabla.(n_e(v_D + v_e)) = 0, \quad \frac{\partial n_i}{\partial t} + \nabla.(n_i v_i) = 0$$
$$m_e n_e\left(\frac{\partial v_e}{\partial t} + (v_D + v_e).\nabla v_e\right) = n_e q_e E - \nabla P_e$$
$$m_i n_i\left(\frac{\partial v_i}{\partial t} + v_i.\nabla v_i\right) = n_i q_i E - K_i(x_i - x_{i0})$$
$$\nabla.E = 4\pi e(n_i - n_e)$$
$$\xi_e = \frac{eE}{m_e\omega^2 - m_e k_x v_D\omega - \frac{k_x^2\gamma T_e\omega}{\omega - k_x v_D}}, \qquad \xi i = \frac{-eE/m_i}{\omega^2 - \frac{K_i}{m_i}}$$

- We use perturbation theory to write the equivalent 1st order equations and use Fourier theory, assuming $A = A_0 e^{i(kx-\omega t)}$form for each perturbed quantity, to solve for the perturbed positions. Substituting into Poisson's equation, gives the dispersion relation

References

[1] G. Mourou, S. Mironov, E. Khazanov, and A. Sergeev, Eur. Phys. J. Spec. Top. 223, 1181 (2014).
[2] T. Tajima, Eur. Phys. J. Spec. Top. 223, 1037 (2014)
[3] T. Tajima and S. Ushioda, Phys. Rev. B 18, 1892 (1978).
[4] X. Zhang, T. Tajima, D. Farinella, S. Youngmin, G. Mourou, J. Wheeler, P. Taborek, P. S. Chen, F. Dollar, and B. Shen, Phys. Rev. Accel. Beams 19, 101004 (2016).

Evolution of the wakefield ($\omega_{TO} = 0$)

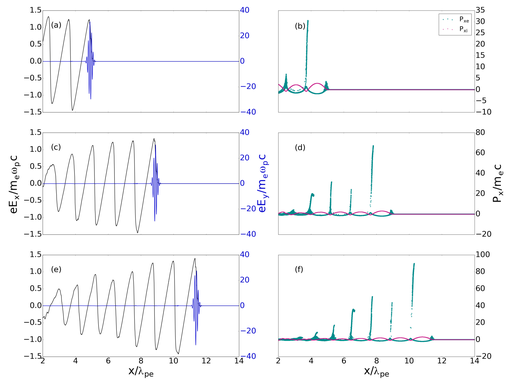

- Evolution of LWFA with $\omega_{TO} = 0$,
  - $\frac{t}{[\lambda_{pe}/2c]} = 10$ (panels a and b)
  - $\frac{t}{[\lambda_{pe}/2c]} = 18$ (panels c and d)
  - $\frac{t}{[\lambda_{pe}/2c]} = 23$ (panels e and f)

Comparison of different lattice force strengths

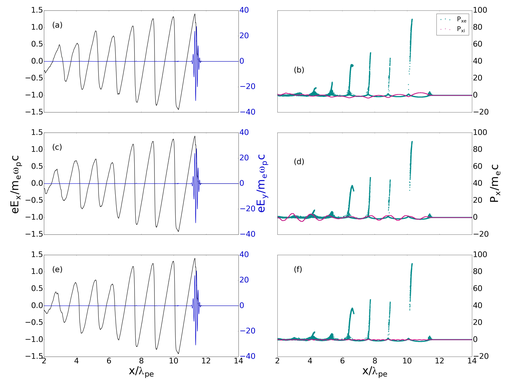

- $\frac{t}{[\lambda_{pe}/2c]} = 23$
- $\frac{\omega_{TO}}{\omega_{pe}} = 0.10$ (panels a and b)
- $\frac{\omega_{TO}}{\omega_{pe}} = 1.00$ (panels c and d)
- $\frac{\omega_{TO}}{\omega_{pe}} = 3.46$ (panels e and f)

- Panels (a), (c) and (e) show electric field of the laser pulse, E_y, shown by blue solid line (right axis) and the longitudinal electric field, E_x, shown by black solid line (left axis) normalized by the Tajima-Dawson field, $E_L^{cr} = \frac{m_e\omega_{pe}c}{e}$.
- Panels (b), (d) and (f) show the phase space for each species. Green stars represent simulation particles with negative charge and red dots represent simulation particles with positive charge. Momentum (right axis) is normalized by $m_e c$, and position is normalized by λ_{pe}.

Simulation of Beam Driven Instability in solids

High ionic frequency

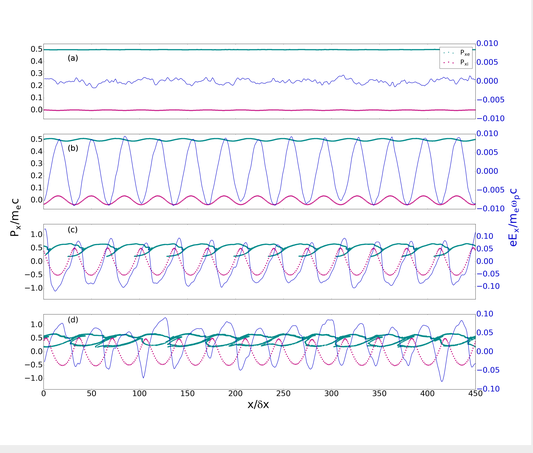

- $\lambda_{observed} \approx 35\times10^{-8}$ cm, $\lambda_{expected} \approx 37\times10^{-8}$ cm
- Evolution of this instability and growth of this mode into a nonlinear phase is shown
- The instability picks up growing linearly and eventually is nonlinearly modulated to form trapped electron orbital characteristic
- Ions display a more harmonic behavior throughout
- Acceleration gradient is $eE_x \approx 0.08 eE_L^{cr} = 80\frac{\text{GeV}}{\text{cm}}$ at $t = 1.2$ fs

Low ionic frequency

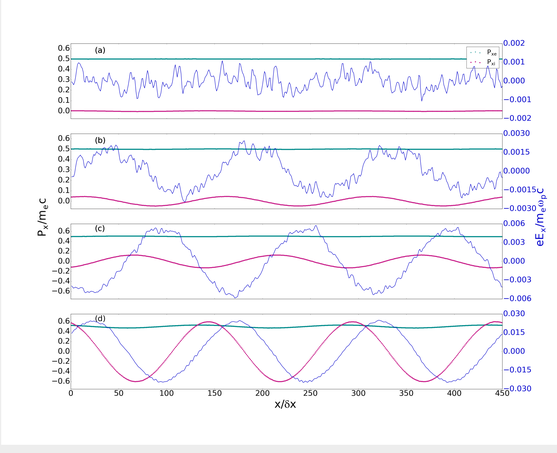

- $\lambda_{observed} \approx 150\times10^{-8}$ cm, $\lambda_{expected} \approx 152\times10^{-8}$ cm
- Evolution of this instability is shown, this instability is so weak that we observe no electron trapping phenomena similar to what has been observed in the low density regime
- v_D was varied (for both high and low ionic frequency cases) and similar characteristics were observed

Simulation setup and Parameters

- Simulations are conducted using the 1D version of EPOCH PIC code
- Ions are manually loaded at the center of each cell (an Å apart from each other)
- Pusher is modified in order to model the lattice force for ions
  - $\frac{dv_n}{dt}\hat{x} = \frac{q}{m}(E + v_n \times B)\hat{x} - \frac{K_i}{m}(x_n - x_{n0})\hat{x}$

- Plasma Density, $n_e = 10^{23}$ cm^{-3}
- $\frac{\omega_{pi}}{\omega_{pe}} = \frac{1}{43}$
- Grid size, $\delta x = 10^{-8}$ cm
- $\delta t = \frac{\delta x}{0.95c} = 3.5\times10^{-19}$ s
- Laser Wavelength, $\lambda_l = 10^{-6}$ cm
- Laser Intensity, $a_0 = 3$
- FWHM, $\frac{\lambda_{pe}}{4} = 2.65\times10^{-6}$ cm
- K_i is varied

Results

- Longitudinal electric field, $E_x \approx 1.4\, E_L^{cr}$
- Acceleration gradient, $eE_x \approx 0.4\frac{\text{TeV}}{\text{cm}}$
- Energy gain, $\epsilon = 100 m_e c^2 = 50\text{MeV}$ ($12\lambda_{pe} = 1.3\times10^{-4}$ cm)
- Maximum electron energy is observed to be $\approx 340\text{MeV}$ in later stages of the simulation and is limited by the pump depletion length
- The wakefield is not affected by the presence of ion modes and negative charges bunched at the end of each bubble continue to gain momentum and energy comparable to the base case with $K_i = 0$
- A noticeable difference in these cases compared to the base case is the presence of an ion mode related to the lattice frequency
- The fundamentals of the LWFA is unaffected

Beam Driven Instability

- Similar plasmons and polaritons (electron plasma waves and ionic plasma modes) can be excited in a solid plasma system with the presence of an electron current[3]
- $\epsilon(k,\omega) = 1 - \frac{\omega_{pi}^2}{\omega^2-\omega_{TO}^2} - \frac{\omega_{pe}^2}{(\omega-k_x v_D^2)^2-k_x^2 v_e^2}$, where v_D is the electron drift velocity

Parameters

High ionic frequency	Low ionic frequency
Plasma Density, $n_e = 10^{24}$ cm^{-3}	Plasma Density, $n_e = 10^{24}$ cm^{-3}
$v_D = 0.5c$	$v_D = 0.5c$
$\frac{\omega_{pi}}{\omega_{pe}} = \frac{1}{2}$	$\frac{\omega_{pi}}{\omega_{pe}} = \frac{1}{63}$
$\frac{\omega_{TO}}{\omega_{pe}} = 3.46$	$\frac{\omega_{TO}}{\omega_{pe}} = 0.11$

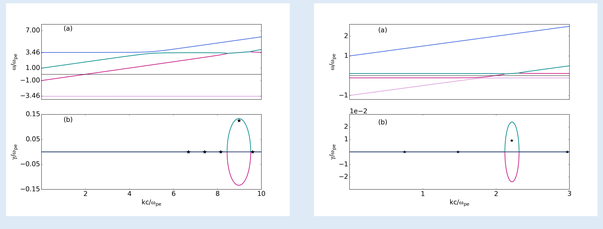

- Solutions to the dispersion equation indicates an unstable mode
- Panel (a) shows the normalized real frequency, ω/ω_{pe}, vs. normalized wavevector, kc/ω_{pe}
- The instability occurs when forward propagating phonon branch crosses the negative energy plasmon branch
- Panel (b) shows the normalized growth rate, γ/ω_{pe}, vs. normalized wavevector
- Stars mark the value of the growth rate found from the simulation data for several modes.